ORIGINAL ARTICLE

Veterinary Research Forum. 2024; 15 (7): 357 - 367
doi: 10.30466/vrf.2024.2014162.4040
Journal Homepage: vrf.iranjournals.ir

Veterinary Research Forum

Preparation and evaluation of controlled released implant containing mesoporous selenium nanoparticles loaded with curcumin in rats with spinal cord injury

Ehsan Lajmiri[1], Moosa Javdani[2], Pegah Khosravian[3], Mohammad Hashemnia[4], Hossein Kazemi Mehrjerdi[1]*

[1] Department of Clinical Sciences, Faculty of Veterinary Medicine, Ferdowsi University of Mashhad, Mashhad, Iran; [2] Department of Clinical Sciences, Faculty of Veterinary Medicine, Shahrekord University, Shahrekord, Iran; [3] Medical Plants Research Center, Basic Health Science Institute, Shahrekord University of Medical Sciences, Shahrekord, Iran; [4] Department of Pathobiology, Faculty of Veterinary Medicine, Razi University, Kermanshah, Iran.

Article Info

Article history:

Received: 31 October 2023
Accepted: 04 March 2024
Available online: 15 July 2024

Keywords:

Chitosan Hydrogel
Curcumin
Spinal cord injury
Selenium nanoparticles

Abstract

In this study, a controlled released delivery drug system designed and synthesized by loading curcumin and selenium nanoparticles (SeNaPs) on chitosan hydrogel, and while evaluating the physicochemical properties of the prepared drug delivery system, the tissue changes caused by the local implant of that system in rats with experimental spinal cord injury (SCI) were investigated. For this purpose, 100 adult female rats were randomly divided into five equal groups which are: Control group without any treatment for SCI, chitosan group that received chitosan hydrogel, curcumin group that received curcumin-loaded hydrogel, SeNaP group that received chitosan loaded with SeNaPs and SeNPCur group that received chitosan loaded with SeNaPs and curcumin. On the 3rd and 7th days of the study, severe infiltration of leukocytes, especially lymphocytes, as well as axon swelling and hemorrhagic necrosis at the lesion sites were observed in all groups, especially the control group. On the 7th day, the severity of these injuries decreased in the SeNPCur group and the highest number of astrocytes was observed in this group. In addition, on the 14th and 21st days of the study, the lowest severity of nerve tissue damage and the lowest presence of inflammatory cells along with the highest number of astrocytes were seen in the SeNPCur group. The glial fibrillary acidic protein study also confirmed the presence of more and significant astrocytes in the SeNPCur, curcumin and SeNP groups at different times of the study, respectively. The histopathological results showed the neuroprotective effects of chitosan hydrogel loaded with selenium and curcumin.

Introduction

Traumatic spinal cord injury (SCI) resulting from the compression of the spinal cord is characterized by two distinct phases in terms of pathology, which are commonly referred to as primary and secondary injuries. In fact, secondary injuries start a few hours after the traumatic (primary) injury and even last for several months. Therefore, the control of secondary injuries is considered as one of the main treatments in SCI.[1,2] One of these therapeutic approaches is the use of nanoparticles with anti-inflammatory and antioxidant potential. Recently, nanoparticles have been extensively studied and used for developing drug delivery systems. The most important advantage of nanoparticle drug is their ability to cross the blood-brain barrier (BBB). The other important advantages of nanoparticle drugs are including great stability, high carrier capacity, incorporation feasibility of both hydrophobic and hydrophilic substances.[3,4]

Selenium (Se) is one of the important trace element and essential micronutrient for the biological functions of humans and animals, and it is required for the prevention and cure of diseases. Therefore, selenium nanoparticles (SeNaPs) have attracted increasing attention due to their improved biological characteristics, as antimicrobial, antiviral, and antioxidant activity along with high bioavailability, low toxicity and high absorptivity in comparison with other inorganic and organic selenium compounds. Likewise, SeNaPs are an effective strategy for the treatment of several neurodegenerative diseases. One of the significant anti-inflammatory mechanisms of SeNaPs is regulated via its influence on the adhesion of monocyte endothelial cells and their penetration into the tissues.[5-7]

***Correspondence:**

Hossein Kazemi Mehrjerdi. DVM, DVSc
Department of Clinical Sciences, Faculty of Veterinary Medicine, Ferdowsi University of Mashhad, Mashhad, Iran
E-mail: h-kazemi@um.ac.ir

Hydrogels have been identified as novel class of three-dimensional networks of functional hydrophilic polymers and are hopeful candidates for drug delivery systems owing to their unique characteristics. Currently, chitosan hydrogels are extensively applied because of their biodegradability, biocompatibility, absorption capacity, inexpensiveness, antimicrobial and non-toxic attributes.[8] According to recent investigations hydrogels as therapeutic scaffolds for central nervous system (CNS) and neural tissue engineering and regeneration have remarkably desirable characteristics. [9,10]

Hydrogels including chitosan hydrogels as biodegradable scaffolds have been shown to significantly inhibit fibrotic scar and cysts formation, decrease the inflammatory response at the site of injury and promote myelin and axonal regeneration. Consequently, chitosan hydrogels are widely used in the preparation and synthesis of drug delivery systems.[11,12] Chitosan, a linear amino polysaccharide shows significant antimicrobial, anti-inflammatory and antioxidant activities. It has been proposed that chitosan can induce growth and differentiation of neural like cells as an external growth factor.[13,14]

The utilization of a chitosan-based hydrogels containing beneficial material such as SeNaPs could be advantageous to facilitate tissue regeneration. Using this approach compounds that play a significant role in guiding and controlling tissue regeneration can be delivered in a controlled manner to the exact site where cell differentiation and proliferation are estimated to take place. Curcumin is a yellow pigment and a low molecular weight polyphenolic compound extracted from the rhizome of *Curcuma longa* L. (turmeric), a flowering plant of the Zingiberaceae family. It has been shown that curcumin, a multifunctional bioactive molecule, significantly induces the spinal cord repair by way of inhibition of glial scar formation and inflammation, therefore, represents a potential treatment for different CNS disorders as SCI. In other words, the efficient extent of curcumin increases the differentiation rate of neural stem cells through Wingless-related integration (Wnt) signaling pathway and induces the differentiation of glioma-initiating cells (GICs).[15] This bioactive substance in turmeric also promotes axonal growth, neuronal development and effectively reduces the activity of reactive astrogliosis and the volume of the lesion cavity. Additionally, curcumin significantly reduces the concentration of the astrocyte biomarker and glial fibrillary acidic protein (GFAP) in the brain.[16,17]

Glial fibrillary acidic protein is a monomeric inter-mediate filament-III protein and discriminatory blood biomarker for numerous neurological disorders such as traumatic brain injury. In humans, this protein is encoded by the GFAP gene.[18] Glial fibrillary acidic protein plays fundamental direct or indirect roles in cell motility, migration and mitosis which is related to the role of GFAP in the growing CNS and in glioma. During cell division by mitosis, the levels of phosphorylated GFAP are increased and moved to the cleavage furrow. GFAP Overexpression, a common characteristics of CNS injury, leads to the formation of aggregates in astrocytes resulting in its usage as a reporter to study the mechanisms that cause gliosis.[18,19] Therefore, the key purpose of current research was to prepare and assess a controlled release implant containing mesoporous SeNaPs bearing curcumin in rats with SCI.

Materials and Methods

Synthesis of curcumin loaded SeNaPs. First, 100 mg of cetrimonium bromide (CTAB; Merck, Darmstadt, Germany) was dissolved to 46.00 mL of distilled water and the mixture was then centrifuged at 800 rpm for 30 min at ambient temperature. After complete dispersion of CTAB, 30.00 mg of zinc was added to the solution and stirred for 12 hr. Then, 2.00 mL of a 5.00 mM sodium selenium oxide solution (Sigma Aldrich, St. Louis, USA) and 2.00 mL of 20.00 mM ascorbic acid solution (Sigma Aldrich) were added and stirred for additional 2 hr. The solution was then centrifuged at 800 rpm for 5 min and washed three times with distilled water and ethanol. The precipitate was dispersed in 30.00 mL ethanol and reflexed at 80.00 ˚C and 800 rpm for 24 hr to remove CTAB. Finally, the 50.00 mg nanoparticles were added to 5.00 mL of a solution containing 50.00 mg curcumin (Sigma Aldrich) and the mixture was stored in a dark place at ambient temperature until further use.[20]

Investigation and comparison of the characteristics of uncoated- and prepared- nanoparticles. The structural characteristics and surface morphology of the synthesized nanoparticles were investigated using a scanning electron microscope (SEM-FESEM; Tescan/Mira, Brno, Czech Republic). Moreover, energy dispersive X-ray (EDX; Tescan/Mira) analysis was utilized to determine the elemental composition of the nanoparticles.

Fabrication of chitosan hydrogels loaded with SeNaPs. For this purpose, 480 mg of pure chitosan was well dispersed in 12.00 mL of 0.10 M acetic acid solution (Merck) and the mixture was allowed to stand without being disturbed at ambient temperature for 3 hr to obtain a homogeneous and clear solution. Afterward, 2.00 mg of the prepared SeNaPs were dissolved in 4.00 mL of distilled water and the mixture was added to the chitosan solution. In a separate container, 3.20 g of β-glycerol phosphate pentahydrate (β-GP; Sigma Aldrich) was dissolved in 2.00 mL of deionized water and the β-GP solution was then added dropwise to the chitosan solution which was placed in an ice bath at 4.00 ˚C for around 10 min (calculated values for the preparation of 16.00 mL of hydrogel for 8 mice).[21]

Morphological and structural characterization of the prepared hydrogel. The prepared sample was frozen directly in a –20.00 ˚C freezer. The frozen sample was then dried in a freeze-dryer. The sample was coated with a thin layer of gold by a sputter coater and the morphological structure of the sample was examined using SEM.[21]

Fourier-transform infrared spectroscopy (FTIR) analysis of hydrogels. The FTIR spectroscopy was employed to identify the functional groups of chitosan and β-GP as well as to investigate the interactions between all the components of the prepared hydrogels. The analysis was performed in the transmission range of 4,000 to 400 cm^{-1}.[21]

***In vitro* release study of nanoparticles-loaded hydrogels.** The amount of 1.00 g of the prepared hydrogel was immersed in 500 mL of phosphate buffer (pH 7.40) under 100 rpm continuous shaking at 37.00 ˚C for up to 30 days. After the 1, 2, 3, 6, 12, 18, and 24 days of incubation a volume of 1.00 mL of sample was removed and 1.00 mL of fresh buffer was added. Finally, release rate of the hydrogels was investigated.[21]

Animal treatments. In the current study, 100 two-month-old female Sprague-Dawley rats weighing 230 to 270 g were used. The animals were randomly divided into five equal groups: 1) The control group (Did not receive any medicine), 2) The chitosan group (Received the chitosan hydrogels), 3) The curcumin group (Received chitosan hydrogels containing curcumin), 4) SeNaP group (Received chitosan hydrogels containing SeNaPs), and 5) The SeNPCur group (Received chitosan hydrogels containing SeNaPs and curcumin). Hydrogels were implanted locally at the site of experimental SCI in different groups. The study protocol was assessed by the Research Committee of the Faculty of Veterinary Medicine and approved by the Research Ethics Committee of Ferdowsi University of Mashhad, Mashhad, Iran (Approval No. IR.UM.REC.1400.330).

Induction of experimental SCI. The rats were anesthetized by an intraperitoneal injection with a mixture of 70.00 mg kg^{-1} ketamine (Alfasan, Woerden, The Netherlands) and 10.00 mg kg^{-1} xylazine (Alfasan).[22] All animals were placed in in the sternal position and the back of the animals (Spine and surrounding area) was clipped and the site was surgically prepared. To induce of SCI, a 2.00 cm skin incision was made between the 8 to 11 thoracic vertebrae using a scalpel blade. After performing a dorsal laminectomy at T8 - T9 level and spinal cord appearance, the aneurysm clips were applied on spinal cords for 1 min to establish standard force for spinal cord compression and induction of SCI. The surgical sites were closed routinely. Paralysis of the hind limbs and tail was considered as a clinical symptom of SCI induction and the efficacy of the spinal cord compression technique. Enrofloxacin (2.50 mg kg^{-1}; Amineh Gostar Co., Tehran, Iran) was administered to all animals for 3 days after surgery.

Histopathological evaluation. Tissue samples were collected from the site of induction of SCI on days 3, 7, 14, and 21 post-surgery following euthanasia of animals with overdose of anesthetics and total dorsal laminectomy of the vertebrae. The collected tissues of all the animals were immersed in formalin 10.00% and sent to the histopathology laboratory. Once routine processing of tissue samples and providing of paraffin blocks, 5.00 µm thick serial tissue sections were cut from the paraffin blocks by a microtome and were stained with Hematoxylin and Eosin (H & E) for standard histopathological examination with a light microscope. Light microscope and H & E staining were used to assess the extent of hemorrhage, tissue necrosis, inflammation and neurological conditions. Furthermore, the spinal cord tissue samples were analyzed by GFAP using immunohistochemistry. The percentage of GFAP-expressing cells was calculated by Image J software (version 1.47; National Institutes of Health, Bethesda, USA).

Statistical analysis. The histopathological results were presented descriptively and the mean ± SD percentage of GFAP expression was compared at the $p < 0.05$ level with one-way analysis of variance among the different groups using SPSS Software (version 23.0; ; IBM Corp., Armonk, USA).

Results

Morphological characteristics of nanoparticles using SEM. The results of SEM displayed that the synthesized SeNaPs were uniformly distributed and circular in shape with a particle size about 200 nm.[6]

Energy dispersive X-ray analysis of nanoparticles. The elemental composition of the prepared nanoparticles was determined by EDX analysis. In the EDX analysis of the nanoparticles, the elements carbon, oxygen, selenium, hydrogen and nitrogen were all detected, and their respective quantities were determined. The results confirmed the presence of SeNaPs, as well as the presence of curcumin and chitosan in the sample (Figs. 1A and 1B).

Morphological characteristics of hydrogels using SEM. The morphological characteristics of chitosan hydrogels and cross-linked chitosan hydrogels were investigated by SEM. The pore size of the chitosan hydrogel were decreased significantly from 10.00 - 20.00 to 5.00 - 10.00 µm in the crosslink chitosan hydrogel indicating effective cross-linking of chitosan with β-GP (Figs. 1C, and 1D).

Characterization of hydrogel structure using FTIR. Figure 2 illustrates the FTIR spectra of the prepared hydrogel samples. As shown in Figure 2A, the band observed at 3,400 cm^{-1} in the spectrum of chitosan was attributed to the presence of N-H, O-H and NH_2 groups.

The peak at the 2,930 cm^{-1} was assigned to the overlap of CH_2 and CH_3 groups. The strong and broad peaks in the range of 11,680 - 1,630 cm^{-1} corresponded to the presence of the amide groups. In addition, the N-H bending vibration of the amines is observed in the region of 1,640 - 1,620 cm^{-1}. The peaks in the range of 2,001 - 1,500 cm^{-1} indicated the bending vibrations of C-H groups. The peak at 1,380 cm^{-1}corresponded to the stretching vibrations of C-O in CH_2-OH group. Also, the area between 1,305 -155 cm^{-1} was attributed to the presence of C-O-C groups in chitosan. Figure 2B illustrates the FTIR spectrum of β-GP. Two characteristic bands at 976 cm^{-1} and 1,069 cm^{-1} were detected in this spectrum. The peak at 976 cm^{-1} indicated aliphatic P-O-C stretching. The band at 1,069 cm^{-1} was attributed to the presence of $-(PO4)_2-$ group and the peak at 920 cm^{-1} was also assigned to the presence of $-(HPO4)_2-$ group. As seen in Figure 2C, no additional characteristic bands were observed in the chitosan + β-GP samples of the system after gelation.

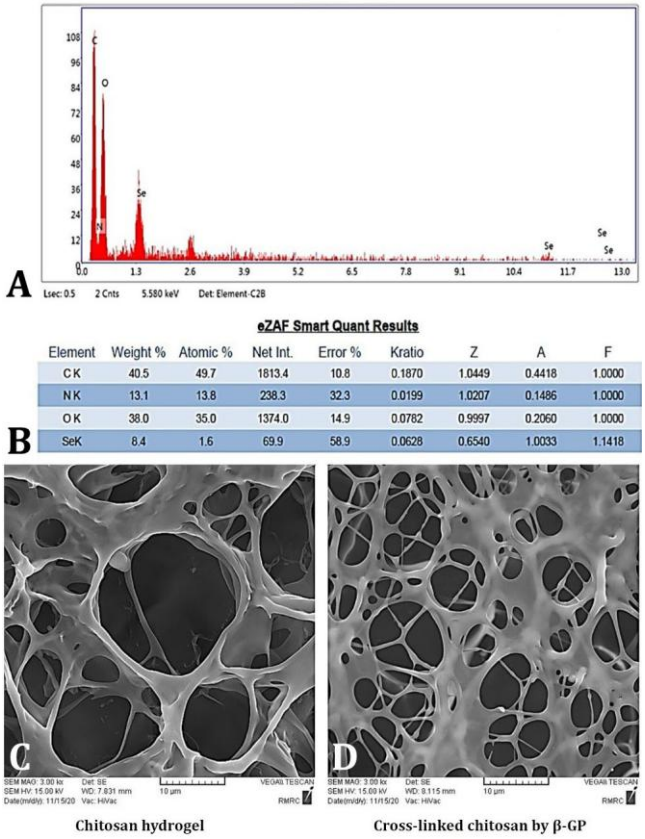

Fig. 1. A) The energy dispersive X-ray analysis of nanoparticles. **B)** The eZAF Smart Quant Results obtained by the EDX analysis gives the weight percentage, atomic percentage, various correction parameters (such as Z-atomic number correction, A-absorption correction, F-fluorescence correction, etc). **C)** Morphological characteristics of chitosan hydrogel and **D)** cross-linking of chitosan by β-GP using scanning electron microscope (3000×).

Changes in this system shifted the stretching groups of C-O and C-O-C at 1,380 and 1,315 cm^{-1} in chitosan to 1,385 and 1,319 cm^{-1}, and the glycerol phosphate pentahydrate groups at 1,073 and 973 cm^{-1} to 1,070 and 366 cm^{-1}. These shifts can be attributed to the electrostatic interaction between the positive charge of the chitosan amino groups and the negative charge of the β-GP phosphate groups. This interaction changes the vibrational modes of functional groups, thereby, caused the observed shifts in the FTIR spectrum.

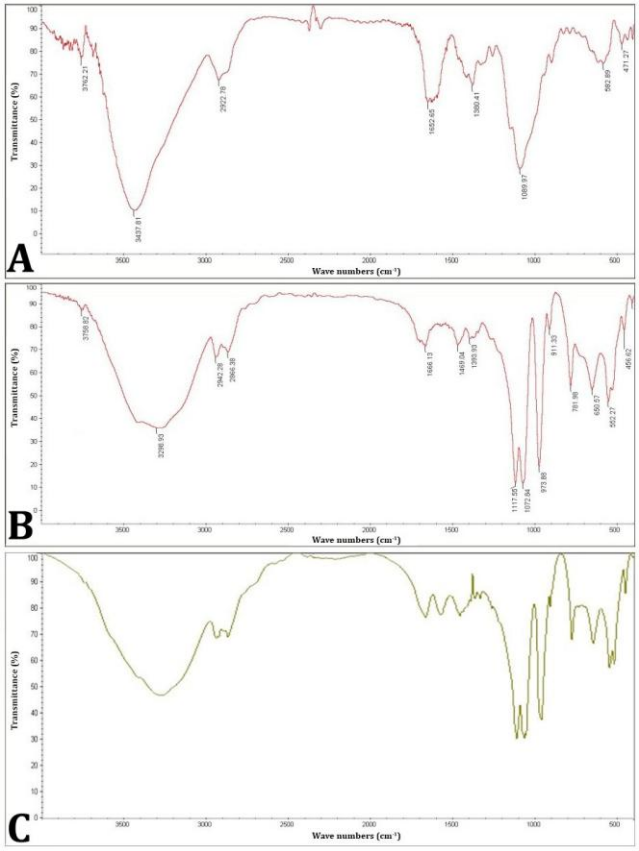

Fig. 2. The fourier-transform infrared spectroscopy spectra of the prepared hydrogel samples including: **A)** chitosan, **B)** β-GP, and **C)** chitosan + β-GP.

Curcumin release profile from curcumin-loaded SeNaPs. Figure 3 illustrates the curcumin release profile from curcumin-loaded SeNaPs in a buffer medium with pH values of 5.50 and 7.40. It is evident that the release of the curcumin was pH-dependent. Additionally, a burst effect was observed within the first 24 hr where there was a rapid release of the active ingredient at both pH values. However, the use of curcumin-loaded SeNaPs was demonstrated to be advantageous in promoting a slow and controlled release of curcumin over time.

Glial fibrillary acidic protein immunoreactivity. The GFAP-positive astrocytes were analyzed in the different parts of gray matter and the means and standard errors were calculated (Fig. 4).

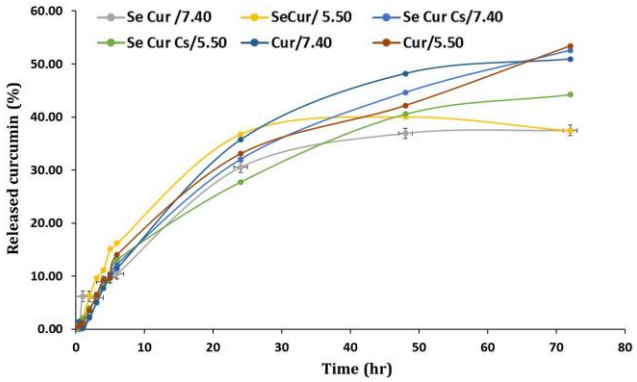

Fig. 3. Curcumin release diagram of selenium nanoparticles at pH 7.40, and pH 5.50, (Se Cur: Selenium nanoparticles + curcumin, Cur: Curcumin, and Se Cur Cs: Selenium nanoparticles + curcumin with chitosan coating).

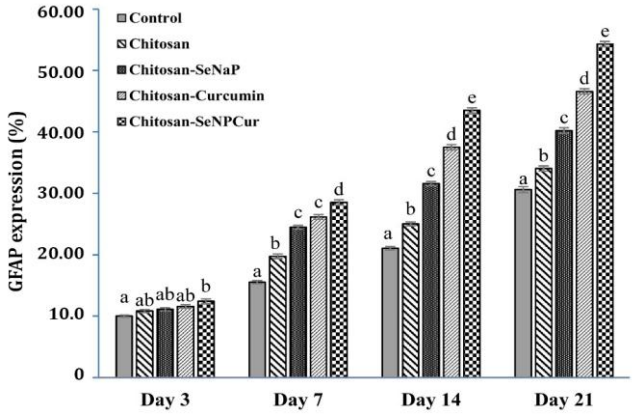

Fig. 4. Mean percentage of glial fibrillary acidic protein (GFAP) expression in each study group.
abcde Different letters in each column indicate a significant difference at $p < 0.05$.

Histopathological examinations on day 3. On day 3 after surgery, severe infiltration of inflammatory cells with a predominance of lymphocytes and less neutrophils and macrophages, axonal swelling, severe hemorrhagic necrosis and edema at the wound site were the main pathological lesions in the control group. The similar lesions were recognized in the treated groups, however, the severity and extent of edema, hemorrhage and inflammation were moderate in these groups. In comparison among treated rats, the severity and extent of the lesions were lower in the SeNPCur group (Fig. 5).

Histopathological examinations on day 7. On day 7 after surgery, the extent of necrotic tissue and edema was found to be lower in the treated groups compared to the control group. Neuronal necrosis and accumulation of inflammatory cells (more macrophages and fewer lymphocytes) were observed in both the control and treatment groups, however, their extent and severity were considerably reduced in the treated groups, particularly the SeNPCur group compared to the control group. At this time, many hypertrophic reactive astrocytes were found surrounding the lesions. Interestingly, the highest number of astrocytes was observed in the SeNPCur group followed by the SeNaP, curcumin, chitosan and control groups, respectively (Fig. 5).

Histopathological examinations on day 14. On day 14 after surgery, the control group exhibited moderate inflammation and neuronal necrosis. Nevertheless, the treated groups demonstrated a prominent reduction in the number of necrotic neurons and inflammatory cells in both the gray and white matters. The SeNPCur group showed a superior therapeutic effect in reducing the severity and extent of necrosis and inflammation compared to the other treated groups. At this stage, reactive astrocytes cluster around the lesion were denser and more mature in the treated groups (Fig. 5).

Histopathological examinations on day 21. On day 21 after surgery, analysis of spinal cord sections of the control group revealed several pathological features such as nerve necrosis, chronic inflammation and fibrosis in the lesion area that surrounded by a dense rim of reactive astrocytes. In the treated groups, minimal infiltration of inflammatory cells at the lesion sites was observed indicating a reduced inflammatory response compared to the control group. The highest number of astrocytes was found in the SeNPCur group in comparison with other treated groups (Fig. 5).

GFAP assessment on day 3. On day 3 after surgery, analysis of immunohistological sections of the gray matter showed no significant increase in the number of GFAP-positive astrocytes in the treated groups compared to control group except for SeNPCur group ($p < 0.05$; Fig. 6).

GFAP assessment on day 7. On day 7 after surgery, a significant increase in the number of astrocytes was observed in SeNPCur group compared to the control group ($p < 0.05$). Hypertrophic astrocytes exhibited a similar distribution pattern in the spinal cord tissue in all exanimated groups. These hypertrophic astrocytes were predominantly detected near the periphery of the spinal cord and around blood vessels (Fig. 6).

GFAP assessment on day 14. On day 14 after surgery, the SeNPCur-treated group displayed the highest number of immunostained astrocytes followed by the curcumin, SeNaP, chitosan and control groups. This indicated that the use of curcumin-loaded SeNaPs (SeNPCur) resulted in the greatest astrocyte activation compared to the other treatment groups. At this stage, reactive astrocytes were characterized as intertwined clusters with long thick cytoskeletal processes (Fig. 6).

GFAP assessment on day 21. On day 21 after surgery, the animals in the SeNPCur group showed the highest percentage of circumscribed areas of reactive astrocytosis. The statistical analysis revealed a significant difference between the treated groups and the control group as well as the SeNPCur group and other treated groups ($p < 0.05$; Fig. 6).

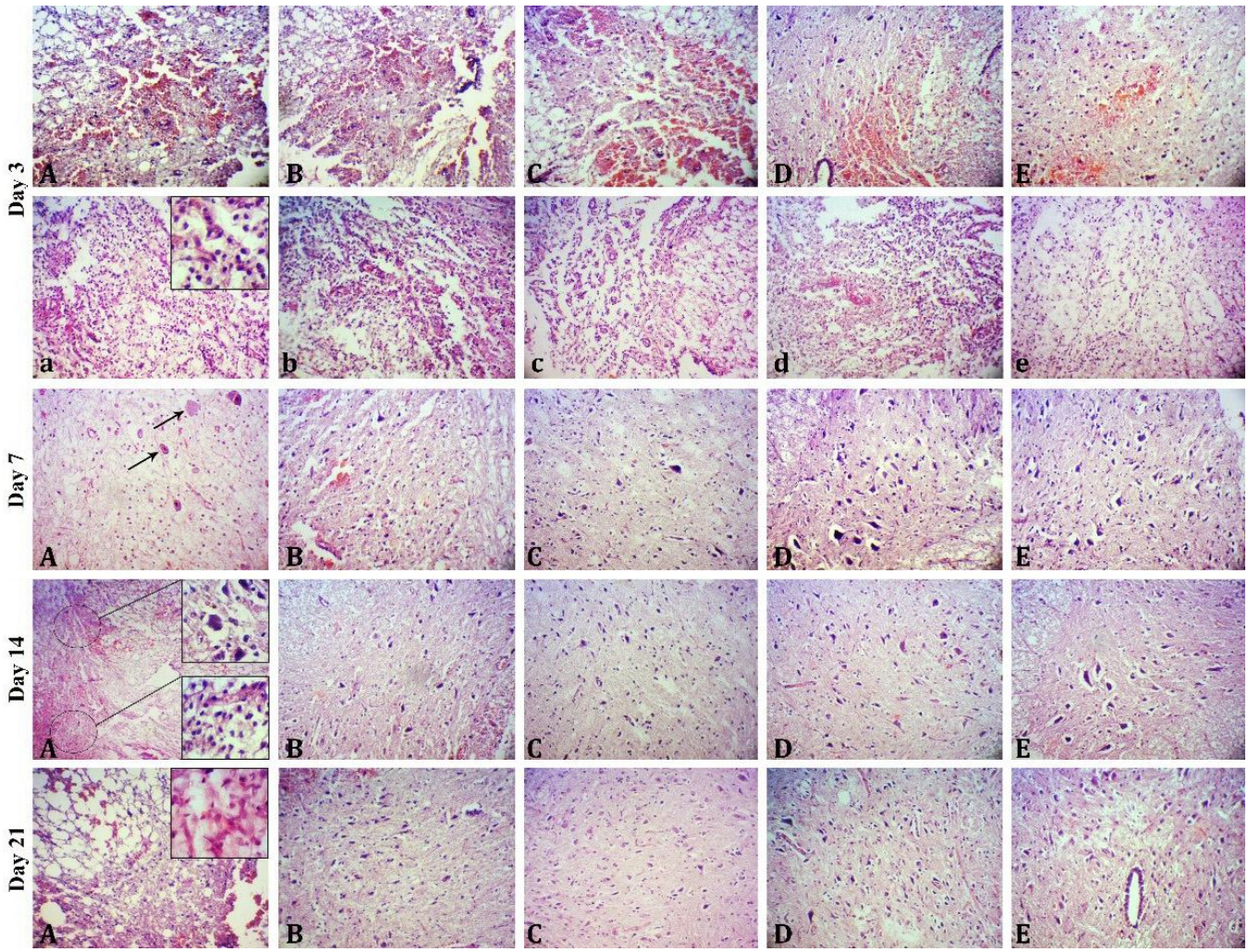

Fig. 5. Sections of the spinal cord of rats subjected to spinal cord injury on days 3, 7, 14, and 21 after surgery in different groups including **A)** control, B) chitosan, **C)** chitosan-SeNaP, **D)** chitosan-curcumin, and **E)** chitosan-SeNaPs-curcumin (Hematoxylin and Eosin staining, 720×). On day 3 post surgery there were severe hemorrhage necrosis **(A)** and severe inflammation **(a)** in the control group and moderate to mild hemorrhage necrosis and inflammation in the chitosan **(B, b)**, chitosan-SeNaP **(C, c)**, chitosan-curcumin **(D, d)** and chitosan-SeNaPs-curcumin **(E, e)** groups. On day 7 post surgery, there were severe neuronal necrosis (arrows) and moderate inflammation in the control group and mild inflammation with a few numbers of neurons with necrotic changes as well as increased dispersed astrocytes in the treated groups, particularly chitosan-SeNaPs-curcumin group. On day 14 post surgery there were moderate inflammation and necrosis in the control group and considerable reduction in the number of dead neurons and inflammatory cells in the treated groups. On day 14 post surgery there were moderate inflammation and infiltration of fibrous tissue in the lesion area in the control group and increase in the number of astrocytes and fibers in the treated groups.

Discussion

In the present study, a controlled release drug delivery system of chitosan hydrogel loaded with SeNaPs and curcumin was used in the experimental model of SCI in rats. Moreover, the histopathological examination was performed on tissue samples obtained from the experimentally induced SCI. The SEM analysis revealed that cross-linked chitosan has more complex networks compared to non-cross-linked chitosan. The formation of these complex networks leads to the development of a controlled release drug delivery system.[23] In fact, the cross-linking technique using β-GP is a physical process that does not form any chemical bonds in it and is confirmed by inspecting the FTIR results of cross-linked chitosan.[22]

Drug delivery into the CNS is an important challenge for the therapy of primary CNS disorders as there are various barriers in the CNS such as the BBB, the blood-spinal cord barrier and the blood-ocular barrier. Because these barriers are the main obstacle in drug delivery to the brain. In fact, the endothelial cells of the BBB prevent paracellular and transcellular transfer of biological substances due to several factors such as the lack of pores, limited endocytic activity, and high metabolic activity.[24]

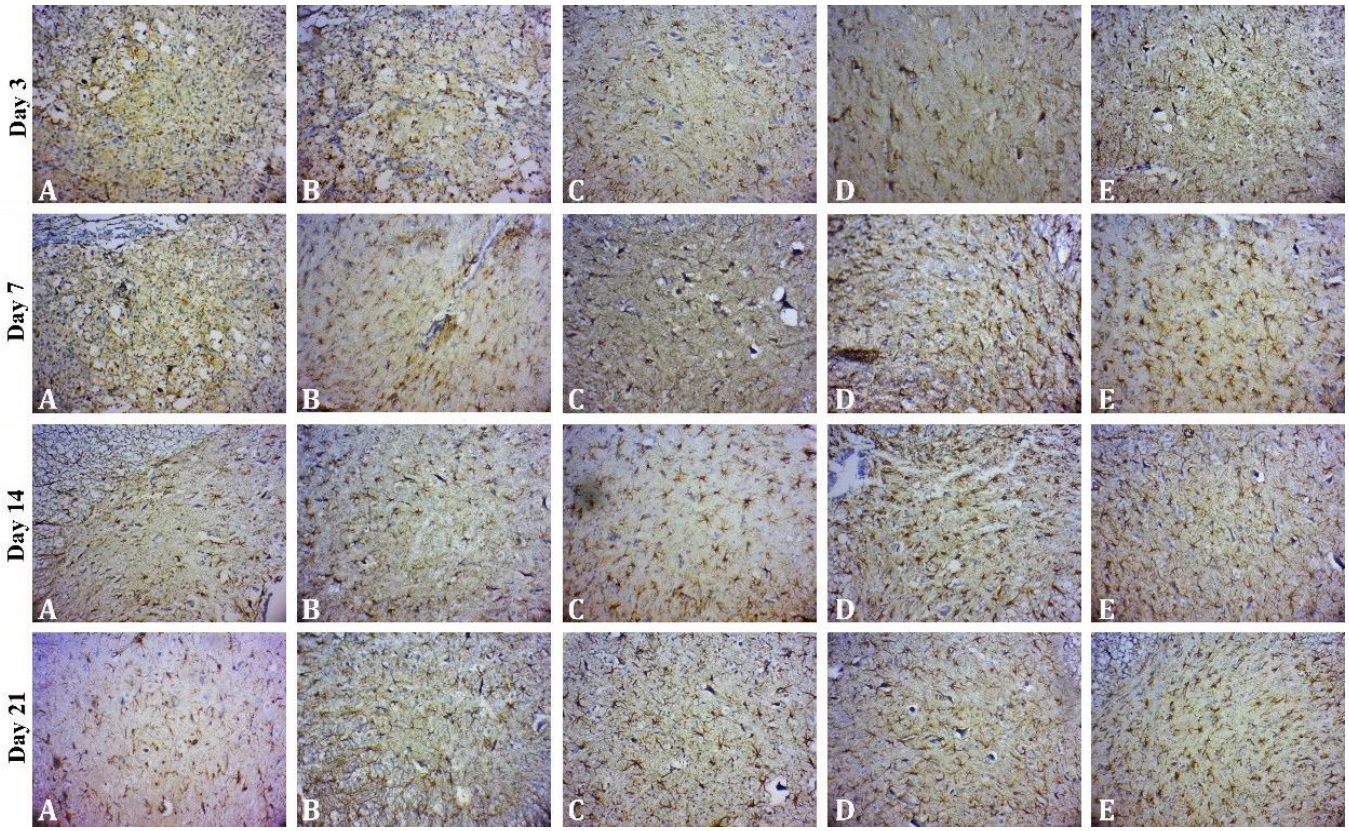

Fig. 6. Expression of glial fibrillary acidic protein (GFAP) in the spinal cord of rats subjected to spinal cord injury on days 3, 7, 14 and 21 after surgery in different groups including **A)** control, **B)** chitosan, **C)** chitosan-SeNaP, **D)** chitosan-curcumin, and **E)** chitosan-SeNaPs-curcumin (Immunohistochemical staining, 720×). On day 3 after surgery, the number of GFAP-positive astrocytes in the chitosan-SeNaPs-group was significantly higher compared to the control group. On day 7 after surgery, hypertrophic astrocytes were predominantly observed near the periphery of the spinal cord and the highest number of cells was observed in the chitosan-SeNaPs-curcumin group. On days 14 and 21 after surgery, the highest number of reactive astrocytes was found in the chitosan-SeNaPs-curcumin group followed by the chitosan-curcumin, chitosan-SeNaP, chitosan and control groups.

The SCI consists of two successive stages: The first stage is characterized by the initial mechanical trauma, SCI and spinal shock. Edema is one of the early symptoms occurring after the primary injury and typically lasts for few days after trauma. The primary immune response consists of the migration and penetration of a broad and diverse range of inflammatory cells into the damaged sites. The second stage occurs within hours to days after the after the initial SCI. Secondary injuries can be further categorized into acute, subacute and chronic phases. The second stage of SCI leads to the significant secrete of inflammatory cytokines, chemokines, matrix metallo-proteinases and growth factors by the immune system.[25-28]

The results of histopathological H & E staining of tissue samples evaluation on the 3rd day of the current study revealed the distinct infiltration of inflammatory cells with the predominance of lymphocytes and a low number of neutrophils and macrophages, axonal swelling, severe hemorrhagic necrosis and edema in the site of SCI in the control group. Immunohistochemical (IHC) analysis of gray matter tissues demonstrated a significant increase in GFAP-positive astrocytes population in the treated groups particularly in the SeNPCur group compared to the control group.

The results of the histological studies demonstrated that chitosan hydrogel loaded with selenium and curcumin nanoparticles reduced the induction of astrocyte expression. Generally, the lack of tissue regeneration and repair observed in the CNS is mainly attributed to the inability of nerve cells to divide and the unfavorable environment for axon-growth promoting factors in the damaged areas which is often caused by gliosis or scar tissue formation. Neural stem cells could be a promising therapeutic approach for the repair of SCI. However, after SCI, endogenous neural stem cells are activated and migrate to the injury sites, where they mostly differentiate into astrocytes, but they seldom differentiate into neurons. Delayed neuronal cell death has been found as a major contributing factor in preventing secondary injuries caused by the destruction of the CNS which reduces the formation of the spinal cord and glial scar.[29]

On the 7th day, the results of H & E histopathological evaluation results demonstrated a decrease in the amount of necrotic tissue and edema in the treated groups compared to the control group. The rate and severity of nerve necrosis and accumulation of inflammatory cells (Leukocytes) in the treated groups, especially the SeNPCur group, were significantly lower than the control group. Furthermore, the SeNPCur group exhibited the highest number of astrocytes followed by the SeNaP, curcumin, chitosan, and control groups in descending order. Histopathological examination of the tissues on the 14th day of the study showed the highest number of stained astrocytes in the SeNPCur group.

The results obtained on the 21st day after SCI indicated a notable decrease in the population of white blood cells in the control group when compared to the SeNaP group. However, there was no significant difference between the other groups. Also, curcumin group exhibited a significant lower lymphocyte population compared to the control, chitosan and SeNPCur groups. However, no significant difference was observed when compared to the SeNaP group. Comparison between different groups presented the highest population of astrocytes in the SeNaP group.

The histopathological results obtained on the 21st day of the study indicated that the SeNPCur group exhibited the highest percentage of limited areas of reactive astrocytosis. Additionally, these finding demonstrated that the treatment groups displayed the lowest levels of the astrocytic intermediate GFAP and the highest percentage of restricted areas of reactive astrocytosis.

Based on the source of the scaffold material, scaffolds are categorized into two groups: natural and synthetic. Several biomaterials have been suggested to build up scaffolds for promoting neural repair. Among them, chitosan scaffolds have been attracting growing interest among both basic and clinical scientists. *In vivo* experimental investigations have shown that chitosan can be used effectively as a promising alternative therapy for nerve tissue repair and regeneration,[30-32] bone regeneration,[33,34] and cartilage tissue repair.[35] In addition, biodegradable nanoparticles stay in the cardiovascular system for an extended period and enable improvement of drug bioavailability by the slow and sustained drug delivery system. Several studies have reported that chitosan can act as a membrane lining and most importantly as a protective agent for neural tissue.[36]

In a study conducted by Javdani *et al*., it was reported that the application of a controlled-release chitosan implant at the site of experimental SCI in rats resulted in improved neuroprotection in the chitosan group compared to the control group.[6] Furthermore, several investigations reported that the administration of slow-release chitosan implants at the site of experimental SCI in rats, led to a reduction in inflammation compared to control groups.[37]

Our findings were consistent with previous studies that showed a better repair in the group treated with chitosan hydrogel compared to the control group. This improvement was probably attributed to the anti-inflammatory activity of chitosan which was consistent with the histopathological results. Recently, growing evidence has suggested that selenium regulates the inflammatory response through multiple mechanisms.[38,39]

Selenium is an important mineral that plays a critical role in keeping an optimal immune response and it effects the innate and acquired immune systems. Adequate levels of selenium have been found to modulate immunological parameters contributing to the proper functioning of the immune system.[7] This essential mineral stimulates the secretion of L-selectin (a member of the selectin family) from monocytes which reduces differentiation into macrophages.[38] Selenium has been shown to offer protection to the injured spinal cord through several mechanisms. It can inhibit inflammation, demyelination of nerve fibers, and neuronal apoptosis, thereby, promoting neuroprotection. Additionally, selenium acts as a scavenger of reactive oxygen species, help reduce oxidative stress and suppress the inflammatory response of SCI secondary injuries.[40,41]

In addition, it has been reported that the local administration of chitosan hydrogel loaded with SeNaPs in rats with experimental SCI leads to healing of the created lesion.[6] Moreover, the histopathological evaluation of the site of the created lesion indicated that the group receiving SeNaPs showed better healing than the control group.Curcumin has been shown to effectively protect spinal cord tissues against oxidative damage. In fact, by neutralizing harmful free radicals and inhibiting oxidative damage, curcumin can help protect the spinal cord tissues from oxidative stress-induced injury.[42] Secondary injuries following SCI can lead to gradual degeneration in the parenchyma of the spinal cord which may eventually result in chronic neuro-degeneration. Inflammation and the generation of oxygen free radicals (also known as reactive oxygen species) play significant roles in the secondary damage that occurs after SCI.[43,44]

Treatment with anti-inflammatories and anti-oxidants,[45] such as SeNaPs and curcumin, has shown promising effects in reducing the damage caused after SCI by reducing oxidative stress. Another possible mechanism of curcumin action for the protection of nerve tissues is its anti-apoptotic properties, prevention of nerve injuries, formation of astrogliosis and glial scar.[17,46] Thus, curcumin exhibits multiple properties that contribute to its therapeutic effects in SCI including antioxidant, anti-inflammatory, anti-apoptotic, and direct neuroprotective properties.[47]

It has been reported that curcumin can improve the motor function recovery and reduce spinal cord edema by

inhibiting the Janus kinase/signal transducer and activator of transcription (JAK/STAT) signaling pathway. The JAK/STAT signaling pathway is involved in various vital biological processes including cell proliferation, apoptosis, differentiation, inflammation and immune regulation.[48] The histopathological results displayed less inflammation and better healing in the curcumin group compared to the control group which provided evidence for the anti-inflammatory and antioxidant activities of curcumin. Previous IHC studies have demonstrated that the presence of reactive astrocytes at the site of injury indicates an improvement in the process of nerve tissue regeneration because astrocytes play diverse roles in the CNS including maintaining BBB integrity, removing toxins and pollutants from the cerebrospinal fluid (CSF), neurotransmitter regulation, metabolic support, ion and pH regulation, cell signaling and neuron communication. The level of activity of astrocytes can be associated with the increased expression of GFAP gene. Glial fibrillary acidic protein is a protein predominantly expressed in astrocytes and its upregulation is commonly used as a marker for astrocyte activation and reactivity.[6]

The present study demonstrated that the group treated with a combination of SeNaPs and curcumin (SeNPCur group) showed the best neuroprotection of spinal cord tissue based on histopathological results. This suggested that the controlled-release form of these compounds because of their anti-inflammatory and antioxidant properties could provide neuroprotective effects after SCI by controlling inflammation and oxidative stress.

Acknowledgments

We thank the Research Deputy of Ferdowsi University of Mashhad, Mashhad, Iran, for the financial supports.

Conflict of interests

The authors declare that they have no conflicts of interest.

References

1. Amanollahi S, Bahrami AR, Haghighitalab A, et al. Immediate administration of hTERT-MSCs-IDO1-EVs reduces hypoalbuminemia after spinal cord injury. Vet Res Forum 2024; 15(1): 27-34.
2. Hafezi B, Kazemi Mehrjerdi H, Moghaddam Jafari A. Effect of captopril on paraplegia caused by spinal cord ischemia-reperfusion injury in rats. Vet Res Forum. doi: 10.30466/vrf.2024.2019729.4126.
3. Singh R, Lillard JW Jr. Nanoparticle-based targeted drug delivery. Exp Mol Pathol 2009; 86(3): 215-223.
4. Tosi G, Costantino L, Ruozi B, et al. Polymeric nanoparticles for the drug delivery to the central nervous system. Expert Opin Drug Deliv 2008; 5(2): 155-174.
5. Sun J, Wei C, Liu Y, et al. Progressive release of mesoporous nano-selenium delivery system for the multi-channel synergistic treatment of Alzheimer's disease. Biomaterials 2019; 197: 417-431.
6. Javdani M, Ghorbani R, Hashemnia M. Histopathological evaluation of spinal cord with experimental traumatic injury following implantation of a controlled released drug delivery system of chitosan hydrogel loaded with selenium nanoparticle. Biol Trace Elem Res 2021; 199(7): 2677-2686.
7. Javdani M, Habibi A, Shirian S, et al. Effect of selenium nanoparticle supplementation on tissue inflammation, blood cell count, and IGF-1 levels in spinal cord injury-induced rats. Biol Trace Elem Res 2019; 187(1): 202-211.
8. Khosravian P, Javdani M, Noorbakhnia R, et al. Preparation and evaluation of chitosan skin patches containing mesoporous silica nanoparticles loaded by doxycycline on skin wound healing. Arch Dermatol Res 2023; 315(5): 1333-1345.
9. Niemczyk B, Sajkiewicz P, Kolbuk D. Injectable hydrogels as novel materials for central nervous system regeneration. J Neural Eng 2018; 15(5): 051002. doi: 10.1088/1741-2552/aacbab.
10. Crompton KE, Goud JD, Bellamkonda RV, et al. Polylysine-functionalised thermoresponsive chitosan hydrogel for neural tissue engineering. Biomaterials 2007; 28(3): 441-449.
11. Chedly J, Soares S, Montembault A, et al. Physical chitosan microhydrogels as scaffolds for spinal cord injury restoration and axon regeneration. Biomaterials 2017; 138: 91-107.
12. Tseng TC, Tao L, Hsieh FY, et al. An injectable, self-healing hydrogel to repair the central nervous system. Adv Mater 2015; 27(23): 3518-3524.
13. Ren YJ, Zhang H, Huang H, et al. *In vitro* behavior of neural stem cells in response to different chemical functional groups. Biomaterials 2009; 30(6): 1036-1044.
14. Yang Y, Liu M, Gu Y, et al. Effect of chitooligosaccharide on neuronal differentiation of PC-12 cells. Cell Biol Int 2009; 33(3): 352-356.
15. Bang WS, Kim KT, Cho DC, et al. Valproic acid increases expression of neuronal stem/progenitor cell in spinal cord injury. J Korean Neurosurg Soc 2013; 54(1): 8-13.
16. Jones EV, Bouvier DS. Astrocyte-secreted matricellular proteins in CNS remodelling during development and disease. Neural Plast 2014; 2014: 321209. doi: 10.1155/2014/321209.
17. Lin MS, Lee YH, Chiu WT, et al. Curcumin provides neuroprotection after spinal cord injury. J Surg Res 2011; 166(2): 280-289.
18. Tykhomyrov AA, Pavlova AS, Nedzvetsky VS. Glial fibrillary acidic protein (GFAP): on the 45th

anniversary of its discovery. Neurophysiology 2016; 48(1): 54-71.
19. Tian R, Wu X, Hagemann TL, et al. Alexander disease mutant glial fibrillary acidic protein compromises glutamate transport in astrocytes. J Neuropathol Exp Neurol 2010; 69(4): 335-345.
20. Verma P, Maheshwari SK. Preparation of sliver and selenium nanoparticles and its characterization by dynamic light scattering and scanning electron microscopy. J Microsc Ultrastruct 2018; 6(4): 182-187.
21. Kiani K, Rassouli A, Hosseinzadeh Ardakani Y, et al. Preparation and evaluation of a thermosensitive liposomal hydrogel for sustained delivery of danofloxacin using mesoporous silica nanoparticles. Iran J Vet Med 2016; 10(4): 295-305.
22. Javdani M, Barzegar A, Khosravian P, et al. Evaluation of inflammatory response due to use of controlled release drug delivery system of chitosan hydrogel loaded with buprenorphine and ketorolac in rat with experimental proximal tibial epiphysis defect. J Invest Surg 2022; 35(5): 996-1011.
23. Qin H, Wang J, Wang T, et al. Preparation and characterization of chitosan/β-glycerophosphate thermal-sensitive hydrogel reinforced by graphene oxide. Front Chem 2018; 6: 565. doi: 10.3389/fchem.2018.00565.
24. Gaillard PJ, Visser CC, de Boer AG. Targeted delivery across the blood-brain barrier. Expert Opin Drug Deliv 2005; 2(2): 299-309.
25. Heller RA, Raven TF, Swing T, et al. CCL-2 as a possible early marker for remission after traumatic spinal cord injury. Spinal Cord 2017; 55(11): 1002-1009.
26. Kwon BK, Stammers AM, Belanger LM, et al. Cerebrospinal fluid inflammatory cytokines and biomarkers of injury severity in acute human spinal cord injury. J Neurotrauma 2010; 27(4): 669-682.
27. Moghaddam A, Child C, Bruckner T, et al. Posttraumatic inflammation as a key to neuroregeneration after traumatic spinal cord injury. Int J Mol Sci 2015; 16(4): 7900-7916.
28. Moghaddam A, Sperl A, Heller R, et al. Elevated serum insulin-like growth factor 1 levels in patients with neurological remission after traumatic spinal cord injury. PloS One 2016; 11(7). e0159764. doi:10.1371/journal.pone.0159764.
29. Jung GA, Yoon JY, Moon BS, et al. Valproic acid induces differentiation and inhibition of proliferation in neural progenitor cells via the beta-catenin-Ras-ERK-p21Cip/WAF1 pathway. BMC Cell Biol 2008; 9: 66. doi:10.1186/1471-2121-9-66.
30. Zhang H, Fang X, Huang D, et al. Erythropoietin signaling increases neurogenesis and oligodendrogenesis of endogenous neural stem cells following spinal cord injury both *in vivo* and *in vitro*. Mol Med Rep 2018; 17(1): 264-272.
31. Nadeem A, Al-Harbi NO, Alfardan AS, et al. IL-17A-induced neutrophilic airway inflammation is mediated by oxidant-antioxidant imbalance and inflammatory cytokines in mice. Biomed Pharmacother 2018; 107: 1196-1204.
32. Yao ZA, Chen FJ, Cui HL, et al. Efficacy of chitosan and sodium alginate scaffolds for repair of spinal cord injury in rats. Neural Regen Res 2018; 13(3): 502-509.
33. Yao NW, Lu Y, Shi LQ, et al. Neuroprotective effect of combining tanshinone IIA with low-dose methylprednisolone following acute spinal cord injury in rats. Exp Ther Med 2017; 13(5): 2193-2202.
34. Chen CK, Chang NJ, Wu YT, et al. Bone formation using cross-linked chitosan scaffolds in rat calvarial defects. Implant Dent 2018; 27(1): 15-21.
35. Sumayya AS, Muraleedhara Kurup G. Biocompatibility of subcutaneously implanted marine macromolecules cross-linked bio-composite scaffold for cartilage tissue engineering applications. Biomater Sci Polym Ed 2018; 29(3): 257-276.
36. Cho Y, Borgens RB. The preparation of polypyrrole surfaces in the presence of mesoporous silica nanoparticles and their biomedical applications. Nanotechnology 2010; 21(20): 205102. doi: 10.1088/0957-4484/21/20/205102.
37. Javdani M, Nafar M, Mohebi A, et al. Evaluation of leukocyte response due to implant of a controlled released drug delivery system of chitosan hydrogel loaded with selenium nanoparticle in rats with experimental spinal cord injury. Tabari Biomed Stu Res 2022; 4(2): 1-16.
38. Duntas LH. Selenium and inflammation: underlying anti-inflammatory mechanisms. Horm Metab Res 2009; 41(6): 443-447.
39. Javdani M, Barzegar A. Application of chitosan hydrogels in traumatic spinal cord injury; A therapeutic approach based on the anti-inflammatory and antioxidant properties of selenium nanoparticles. Frontiers Biomed Technol 10(3): 349-369.
40. Kim JW, Mahapatra C, Hong JY, et al. Functional recovery of contused spinal cord in rat with the injection of optimal-dosed cerium oxide nanoparticles. Adv Sci 2017; 4(10): 1700034. doi: 10.1002/advs.201700034.
41. Gao Y, Vijayaraghavalu S, Stees M, et al. Evaluating accessibility of intravenously administered nanoparticles at the lesion site in rat and pig contusion models of spinal cord injury. J Control Release 2019; 302: 160-168.
42. Sahin Kavakli H, Koca C, Alıcı O. Antioxidant effects of curcumin in spinal cord injury in rats. Ulus Travma Acil Cerrahi Derg 2011; 17(1): 14-18.
43. Dumont RJ, Okonkwo DO, Verma S, et al. Acute spinal cord injury, part I: pathophysiologic mechanisms. Clin Neuropharmacol 2001; 24(5): 254-264.

44. Sanli AM, Turkoglu E, Serbes G, et al. Effect of curcumin on lipid peroxidation, early ultrastructural findings and neurological recovery after experimental spinal cord contusion injury in rats. Turk Neurosurg 2012; 22(2): 189-195.
45. Christie SD, Comeau B, Myers T, et al. Duration of lipid peroxidation after acute spinal cord injury in rats and the effect of methylprednisolone. Neurosurg Focus 2008; 25(5): E5. doi: 10.3171/FOC.2008.25.11.E5.
46. Lin MS, Sun YY, Chiu WT, et al. Curcumin attenuates the expression and secretion of RANTES after spinal cord injury *in vivo* and lipopolysaccharide-induced astrocyte reactivation *in vitro*. J Neurotrauma 2011; 28(7): 1259-1269.
47. Yao M, Yang L, Wang J, et al. Neurological recovery and antioxidant effects of curcumin for spinal cord injury in the rat: a network meta-analysis and systematic review. J Neurotrauma 2015; 32(6): 381-391.
48. Zu J, Wang Y, Xu G, et al. Curcumin improves the recovery of motor function and reduces spinal cord edema in a rat acute spinal cord injury model by inhibiting the JAK/STAT signaling pathway. Acta Histochem 2014; 116(8): 1331-1336.